ROBUST TRACKING PERFORMANCE ENHANCEMENT THROUGH UNCERTAINTY DIVISION

M. Gil-Martínez[1], M. García-Sanz[2]

[1]System Engineering and Automation Group, Electrical Engineering Department, University of La Rioja.
Luis de Ulloa, 20, 26004 Logroño, SPAIN. Fax:+34 941 299478. E-mail: montse.gil@die.unirioja.es

[2]Automatic Control and Computer Science Department, Public University of Navarra.
Campus Arrosadía, s/n, 31006 Pamplona, SPAIN. E-mail: mgsanz@unavarra.es

Keywords: Robust Control, Quantitative Feedback Theory, Uncertain systems.

Abstract

When the process uncertainty size increases, even linear minimum phase systems must sacrifice desirable aggressive feedback control benefits to avoid an excessive 'cost of feedback', while preserving the robust stability. With a suitable uncertainty division and a QFT controller-prefilter to command each uncertainty subset inside a controller-scheduler structure, it is possible to enhance the feedback tracking performance without an excessive bandwidth. To preserve the robust stability from any failure in the switching, each controller is designed to be stable in the whole uncertainty domain, and as accurate in command tracking as desired in its uncertainty subset.

1 Introduction

The feedback control is only justified to reduce the closed loop sensitivity to any kind of uncertainty, in the plant modeling or in the unmeasurable disturbances [11]. Thus, the amount of feedback is directly proportional to the amount of uncertainty and to the sensitivity reduction required. Besides, a unique controller can not perform as well for a wide uncertainty plant set as for a smaller domain of uncertainty.

The feedback trade-offs derived from performance limitations in uncertain systems have been widely discussed in the control literature [3][4][14]. The Quantitative Feedback Theory (QFT) stands out for its transparency and the quantitative formulation of the feedback limitations [13][17]. Let's consider the open loop transmission function (controller plus plant): $L(j\omega)=G(j\omega)P(j\omega)$. Sufficiently large feedback (i.e. $|L|>>|P|$) removes the effect of the plant ignorance and of the disturbances. On the other hand, any practical $L(j\omega)$ must go to zero as $\omega\to\infty$, but robust stability requires that $|L|$ decreases comparatively slowly with ω, [5]. Consequently, there is an intermediate frequency range where the excessive open-loop bandwidth due to feedback benefits amplifies dangerously sensor noises or supposedly negligible disturbances, mainly at the plant input [12]. This effect, called the 'cost of feedback' [11], produces elements of G and P to be saturated most of the time, such that the useful signal components due to input commands cannot get through [12].

In this context, the existence of a unique controller that meets simultaneously different nature control requirements was discussed in [9]. Considering the plant uncertainty inherent to the system and the maximum bandwidth limited by the expected level of noise at plant actuators, a suitable selection of the feedback specification values taking into account the trade-offs was analyzed in [8]. However, for high plant ignorance or highly noise environments, this may imply a poor performance.

Therefore, the uncertainty reduction remains as the only solution. An infinite uncertainty division translates into adaptive control schemes where a particular controller is responsible for a unique plant identified in the uncertain domain. Despite of vigorous research in the field of adaptive control, rather few practical applications have appeared [2]. The reasons seem to be that stability of the closed loop is difficult to guarantee during parameter adaptation. Some interesting attempts of comparing and mixing robust and adaptive principles were made in [1] [10] [16]. A first attempt to develop a methodology for the uncertainty division in the QFT domain is presented in [7]. This work studied the uncertainty contribution at the lowest frequency QFT bound, from the graphical arrangement of the M-contours and the lowest-frequency template in the Nichols Chart (NC). The purpose was to reduce the controller static gain.

This paper shows the feedback tracking control limitations due to the uncertainty size in LTI m.p. plants. These are discussed from the QFT bounds, computed with the formulas developed in [6] and broadly studied in [9] [8]. The goal is to divide the uncertainty. Then, several controllers will improve the feedback benefits and minimize the cost of feedback in their uncertainty subset. The whole structure should be a nonlinear controller scheduler [15] that would switch the controllers through on-line measurements of certain auxiliary variables. To preserve robustness despite of failure in the switching, each controller will be designed robustly stable for the full uncertainty.

This paper consists of five sections. Section 2 deals with the nature and severity of the QFT bounds. Section 3 details the

difficulties in the open loop transmission loop shaping, revealing the limitations in the tracking feedback performance. Section 4 illustrates the improvements of the uncertainty division through a practical example. Finally, Section 5 contains the conclusions.

2 Feedback Control Requirements and Bound Typologies in QFT

Let's consider the feedback control scheme in Fig.1. General feedback control specifications are formulated in terms of QFT (see the 1st column in Table I) imposing maximum tolerance models $\delta_k(\omega)$ on the magnitude of certain transfer functions $|T_k(j\omega)|$, k=1,...,M, from some inputs to some outputs in the frequency domain [17]. Then, the controller $G(j\omega)$ design methodology translates these frequency domain specifications of an uncertain feedback system into *bounds* on the NC that the nominal loop transmission $L_0(j\omega)$ must meet. Therefore, the bound arrangement is the key point in the controller synthesis process.

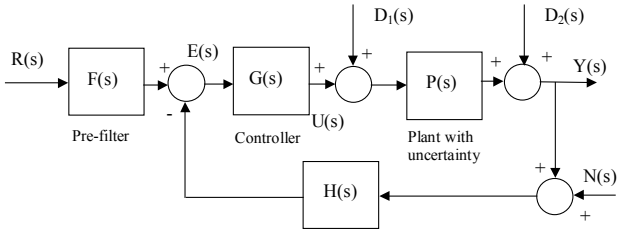

Fig 1. General MISO feedback control scheme

General Feedback Control Inequalities (All magnitudes depends on ω)	*Specification Value*	*Bound Typology*
$\|T_1\| = \left\|\frac{U}{D_1}\right\| = \left\|\frac{Y}{N}\right\| \le \delta_1$	$\delta_1 < 1$	Lower
	$\delta_1 > 1$	Outer
$\|T_2\| = \left\|\frac{Y}{D_2}\right\| \le \delta_2$	$\delta_2 < 1$	Upper
	$\delta_2 > 1$	Outer
$\|T_3\| = \left\|\frac{Y}{D_1}\right\| \le \delta_3$	$\delta_3 < p$	Upper
	$\delta_3 > \{p\}$	Outer
$\|T_4\| = \left\|\frac{U}{D_2}\right\| = \left\|\frac{U}{N}\right\| = \left\|\frac{U}{RF}\right\| \le \delta_4$	$\delta_4 < p$	Lower
	$\delta_4 > 1/\{p\}$	Outer
$\delta_{5\inf} < \|T_5\| = \left\|\frac{Y}{R}\right\| \le \delta_{5\sup}$, $\left\|\frac{T_5}{F}\right\| \le \delta_5 = \frac{\delta_{5\sup}}{\delta_{5\inf}}$	$\delta_5 < p_{max} / p_{min}$	Upper
	$\delta_5 > p_{max} / p_{min}$	Outer

Table I. Bound Typologies for General Feedback Specifications

The bound typology [9] refers to the bound appearance and the way to achieve the bound. Fig. 2 depicts general bound typologies for general feedback control specifications such as those studied in [9] that are summarized in Table I (3rd column). The necessary trade-offs among conflicting requirements are discussed in the QFT bound domain in [9], and outlined below.

When an *upper* bound occurs, L_0=GP_0 must be placed on or above it, and is usually depicted as a *continuous* line (see Fig.2b). These upper bounds look for a minimum gain $|L_0|$ at the whole phase range [-2π 0] rad, which must be added to P_0 by the controller G. Sufficiently large feedback, $|L|>>|P|$, removes the effect of P ignorance and of the disturbances. The bounds with this typology should become dominant at low-medium frequencies demanding the robust feedback benefits: the input and output disturbance rejection and the command tracking (sensitivity reduction).

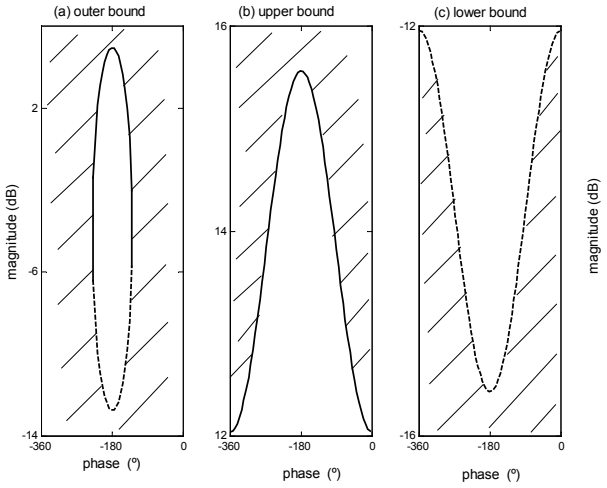

Fig. 2. QFT bound typologies

The *outer* bounds (Fig.2a) enclose the critical stability point 0 dB∠-π rad, building a forbidden area all around that must not be penetrated by L_0. This ensures certain minimum gain and phase margins [17] including the uncertainty. When there are no *lower* bounds (discussed below), the robust stability *outer* bounds become relevant at medium frequencies and dominant in the high frequency band. As long as any practical L must go to zero as $\omega\to\infty$, the outer bounds constrict the gain $|L_0|$ decrement ratio with increasing frequencies in such a way that robust stability principles are met according to Bode's Integrals [5].

Due to $|L|$ decreasing comparatively slowly with ω, there is an intermediate range where $|L(j\omega)|<<1$ but $|L/P\ (j\omega)|>1$. That means a dangerous amplification of the noise N at Y and U. Satisfyingly small output deviations can be achieved with available instrumentation. However, large $|L/P|$ peaks produce unavoidable large U peaks [12], this being the main price paid for feedback, also referred in QFT as the 'cost of feedback' [11]. A large cost may produce elements of G and P to be saturated most of the time, in such a way that the useful signal components due to input commands cannot get through.

Then, once the feedback benefits are won at the low-medium frequencies, the open-loop gain of L=GP should decrease with the frequency as quick as possible. It can be taken into account in the QFT controller design in two ways. Firstly, when relaxing the main feedback objectives that previously gave *upper* bounds at the low frequencies, they yield now non-dominant (respecting to stability) outer bounds. Then, L_0 can be loop-shaped looking for its high frequency asymptote. The $|L_0|$ decrement ratio is only limited by the robust stability *outer* bounds. Another way to guarantee a low enough high frequency gain consists in the *explicit* formulation of robust specifications to cut it off. Then, the *lower* bounds (Fig. 2c) restrict the gain $|L|$ to a maximum at each phase in [−2π 0] rad, and are usually depicted as a *discontinuous* line. This bound typology should become dominant just at high frequencies, avoiding its incompatibility with the low-medium frequency *upper* bounds.

3 Performance Limitations in Tracking

The bound arrangement on the NC shows quantitatively the limitations in the feedback performance. Let's consider for example Fig. 3(a), where robust tracking and stability specifications are represented by QFT bounds. It is assumed that the desired robust tracking performance basically configures the *upper* bounds at the lowest frequencies, i.e. $B(j0.1)$, $B(j1)$. At these frequencies, the open loop magnitude uncertainty, p_{max}/p_{min}, should be reduced under a threshold $\delta_T=\delta_{Tsup}/\delta_{Tinf}$ that represents the reduction in the closed loop uncertainty, $\{|L/(1+L)|\}<\delta_T$. Then, $p_{max}/p_{min}>\delta_T$, and upper bounds result according to Table I. p_{max} and p_{min} represent the maximum and minimum magnitude plants of the ω-template $\{P(j\omega)\}=\{p(\omega)\angle\theta(\omega)\}$.

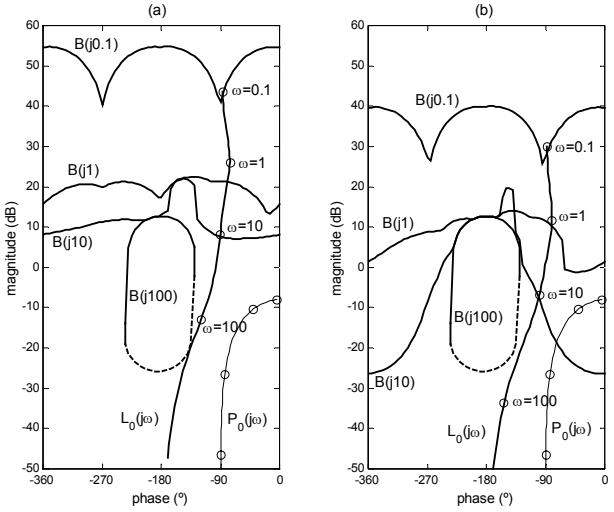

Fig. 3. Bound arrangement and loopshaping for (a) certain plant uncertainty and certain tracking and stability requirements; (b) the same plant uncertainty and robust stability but poorer tracking performance.

From medium frequencies onward, the robust stability requirements become significant too in Fig. 3(a). Stability requirements constraint complementary sensitivity function such that $|L/(1+L)|<\delta_S$. Being $\delta_S=1.3$ ensures minimum stability margins of 45º and 4.9dB [17]. As discussed in [8], $\delta_S<<1$ in stability terms implies too conservative margins, and $\delta_S>>1$ highly, underdamped systems. According to Table I, $\delta_S>1$ implies outer bounds and, as long as δ_S is close to the unity, these outer bounds become dominant at high frequencies.

Hence, the upper bound $B(j10)$ in Fig. 3(a) is the less favorable intersection between the upper bound due to $\{|L/(1+L)|\}<\delta_T$ (main contribution) and also the outer bound due to $|L/(1+L)|<\delta_S$ (note the peak close to -2π rad), resulting in an upper bound intersecting both. The high frequency is dominated exclusively by the stability outer bound, $B(j100)$. The specific plant uncertainty values and the tracking and stability tolerances to built Fig. 3 are studied through the example in Section 4. The loop-shaping difficulties stemming from the bound outlook are discussed below.

A proper tracking accuracy in the static behavior –zero steady state error– requires adding a pole at the origin 's', if there is no one in the plant P. Afterwards, the required open-loop static gain K_{dc} is added to fulfill the lowest frequency bound, i.e. $B(j0.1)$. And subsequently, poles and zeros are added to meet the frequency bounds along the frequencies and to try to reach the high frequency asymptote as soon as possible (cost of feedback minimization).

Therefore, the higher the lowest frequency bound $B(j0.1)$, the larger the static gain K_{dc} needed. And this has an unavoidable drawback effect on the high frequency range. $L_0(j\omega)$ necessarily increases at the whole frequency range, since a desired rapid decrement (more excess of poles over zeros) of $|L_0|$ from medium to high frequencies, $\omega>\omega_I=10$, is impracticable due to the high frequency stability *outer* bound, i.e. $B(j100)$, and also due to the fixed Bode's relation phase-magnitude [5]. To show clearly this effect, take out $B(j1)$ and $B(j10)$, i.e. let's consider just $|T(j\omega_T)|<\delta_T(\omega_T)$, $\omega_T=0.1$ rad/s and $|T(j\omega_S)|<\delta_S(\omega_S)$, $\omega_S=0.1$, 100 rad/s. Fig. 4 shows the effect of raising the upper bound of the lowest frequency ω_{lf}, e.g. $B(j0.1)$, exclusively owed to $|T(j\omega)|<\delta_T(\omega)$, $\omega=0.1$. Compare Figs. 4(a) and 4(b). The same control structure is used in both loop shapes: L_{0a} and L_{0b} are obtained adding a pole at the origin, then certain static gain K_{dc}, plus a zero z, and finally a pole p. Fig. 4 clearly reveals how the $|L_0(j\omega_{lf})|$ increment to satisfy the higher $|B(j\omega_{lf})|$ is paid with a high gain excess $|L_0(j\omega_{hf})|$, i.e. a major cost of feedback. A major control effort peak is also solicited to actuators.

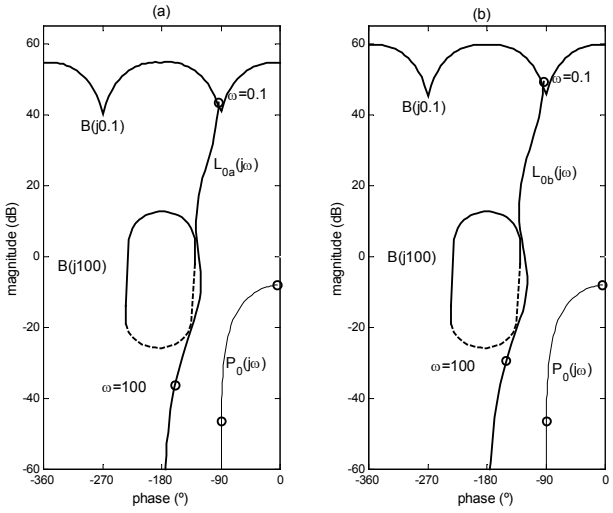

Fig. 4. Increment of the low and high frequency open loop gain $|L|$ for more accurate low frequency tracking in (b) compared to (a).

The situation is much more complex if stringent tracking bounds appear at mid frequencies, e.g. the upper $B(j1)$ and $B(j10)$ bounds in Fig. 3(a). Now a zero closer to the origin than that in Fig. 4(a) is needed to increase the gain $|L_0|$ and meet the upper $B(j10)$ bound. The extra $|L_0|$ increase due to the pairs zero-pole demanded by the mid-frequency tracking performance is added to the static gain required by the lowest frequency tracking performance. And both contribute to increase the cost of feedback in the high frequency range, e.g. $\omega\geq100$. A harder $B(j1)$ bound would have lead to add extra pairs zero-pole, increasing the controller complexity. For the

same excess of poles over zeros required, each extra zero requires an extra pole. Then, the complexity of the controller is translated into significant delays to apply the expected control signal, at least in practice.

Hence the 'cost of feedback' and the controller complexity increase due to tougher tracking bounds at any frequency $\omega \leq \omega_T$, and especially at the lowest frequency. The drawback gets even worse for non-minimum phase plants, for unstable plants and/or for plants with delays, where the decrement ratio of L_0 is more constricted.

A constraint looking for certain maximum open-loop gain at the high frequency, $\max|L_0(j\omega_{hf})|$, could be explicitly expressed. Then, explicit robust specifications on certain closed-loop transfer functions that yield lower bounds are suggested (see Table I). For simplicity reasons, this paper just imposes implicit conditions such as a maximum $|L_0(j\omega_{hf})|$ on the loop-shaping step. Then, certain upper bounds due to robust tracking specifications at low-mid frequencies could be incompatible with a high frequency gain $|L_0(j\omega_{hf})|$ under a threshold. For example, Fig. 3(a) expresses the impossibility of meeting the bounds depicted and simultaneously guaranteeing $|L_0(j\omega_{hf}=j100)|$ under –20dB. This is due to the $B(j10)$ height of about 10dB, being impossible to decrease $|L_0|$ from 10dB to –20dB in just one decade without penetrating the outer robust stability bound $B(j100)$.

The tracking bound arrangement is due to both, the hardness of sensitivity reduction $\delta_T(\omega)=\delta_{Tsup}/\delta_{Tinf}(\omega)$ and the plant uncertainty $\{P\}$. Then, an achievable feedback control can be guaranteed by a proper selection of $\delta_T(\omega)$ as [8] demonstrated. The problem comes down to relaxing appropriately $\delta_T(\omega)$, supposing that $\{P(\omega)\}$ is unchangeable. An example for the new situation is depicted in Fig. 3(b), where the upper bounds $B(j0.1)$, $B(j1)$, $B(j10)$ reduce their height allowing to place $|L_0(j\omega_{hf}=j100)|$ under –20dB. However, this could imply a poor tracking performance, whether $\delta_T(\omega)$ would get close to $p_{max}/p_{min}(\omega)$. Then, the solution requires the reduction of the uncertainty to get a similar bound distribution than that in Fig. 3(b), but without having to relax δ_T, and therefore the desired performance remains and can be even more ambitious. As long as the uncertainty is inherent to the system nature, the only way out is to divide the uncertainty and to control each division with a low cost controller, preserving the stability robustness. The methodology is described through an example.

4 Example of Uncertainty Division

Let's consider a dc field-controlled motor whose nominal characteristics are those in Table II. Assuming that the angular velocity Ω is the plant output to be controlled, manipulating the field voltage V_f, the dc motor in Laplace terms obeys:

$$P(s) = \frac{\Omega}{V_f} = \frac{K_m / R_f}{sJ + b} = \frac{K}{sJ + b}, \qquad (1)$$

where the electrical time constant L_f/R_f has been neglected compared to the field time constant J/b (see Table II). Usually the motor parameters differ from the nominal ones due to temperature and some other special effects. Because of that, in this example it is supposed a 20% variation in b and a 5% deviation in $K=K_m/R_f$ from their nominal values. In addition, the larger divergence observed in the proposed real application takes place at the rotor inertia J. Its nominal value of J=0.01 refers to unload driving. However, considering the load, J is expected in [0.01 0.1] between unload and full load.

Parameter	Nominal Values
Unload Rotor Inertia, J	0.01 kg m^2
Friction, b	0.1 N m s
Motor constant, K_m	0.05 N m /A
Field Resistance, Rf	1 Ω
Field Inductance, Lf	<<0.1 H

Table II. Nominal Characteristics of a Dc Field-Controlled Motor

The speed control requirements in QFT terms are *(i)-(iii)*:

(i) Robust stability with minimum margins of $MF \geq 45º$ and $MG \geq 4.9$dB. QFT expresses it like: $|L/(1+L)| < \delta_S$, $\delta_S(\omega_S)=1.3$, $\omega_S \in [0, \infty]$ rad/s. Discretising the frequency vector: $\omega_{iS}=\{0.1, 1, 10, 100\}$ rad/s.

(*ii*) Robust tracking performance, $\delta_{Tinf} < |F \cdot L/(1+L)| < \delta_{Tsup}$, at $\omega_T \leq 10$ rad/s, being the upper and lower tracking models:

$$\delta_{T\sup}(s) = 0.66(s+30)/(s^2+4s+19.75) \qquad (2)$$

$$\delta_{T\inf}(s) = 8400/(s+3)(s+4)(s+10) \qquad (3)$$

For the tracking frequency range: $\omega_{iT}=\{0.1, 1, 10\}$ rad/s, the specification values from (2) and (3) result $\delta_T=\delta_{Tsup}/\delta_{Tinf}=\{1.0012, 1.1255, 3.0771\}$. Note that for the G design the prefilter F is omitted, and then $\delta_{Tinf} < F \cdot L/(1+L) < \delta_{Tsup}$ translates to $L/(1+L) < \delta_T$ [17].

(*iii*) A low enough high frequency open-loop gain to reduce the 'cost of feedback', e.g. $|L(j\omega_{hf})| <$ -20dB, $\omega_{hf} \geq 100$.

Considering the parameter uncertainty defined and $\omega_i=\{0.1, 1, 10, 100\}$ rad/s for the frequency vector, Fig. 5 depicts the plant templates. Note the huge phase and magnitude uncertainties of the templates $\{P(j1)\}$ and $\{P(j10)\}$. The low and high frequency templates, $\{P(j0.1)\}$ and $\{P(j100)\}$, mainly display magnitude uncertainty.

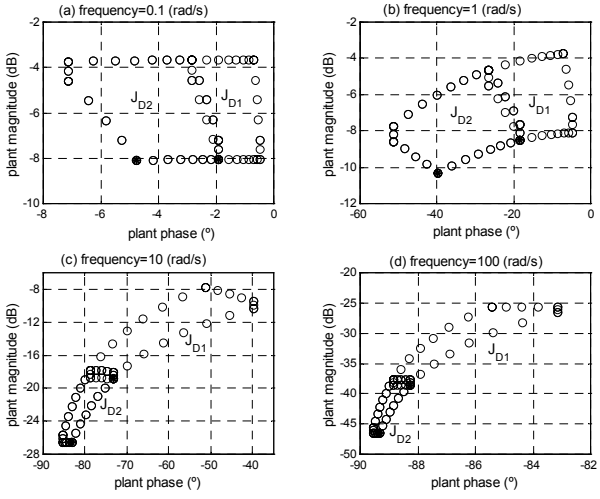

Fig. 5. Plant templates for the full and divided parameter uncertainty

The QFT bounds expressing the stated robust specifications (*i*)-(*iii*) were depicted in Fig. 3(a). The bound typology and its severity according to the uncertainty and the specification models were discussed in Sections 2 and 3. The loop-shaping $L_0=GP_0$ performed on the bound arrangement yields:

$$G_{T1}(s) = 37.71\left(\frac{s}{0.1}+1\right)\Big/ s\left(\frac{s}{175.5}+1\right) \quad (4)$$

The prefilter F to place $|L/(1+L)|$ in-between δ_{Tsup} and δ_{Tinf} :

$$F(s) = 28/\left(s^2+11s+28\right) \quad (5)$$

According to Fig. 3(a), it is impossible to loop-shape a controller that meets explicit bounds on stability and tracking specifications in (*i*) and (*ii*), and that cuts off simultaneously the implicit cost of feedback in (*iii)*. This performance limitation was argued in Section 3. Figs. 6(a,b) simulate the time domain performance of the designs (4) (5) for the plant: $J=J_{max}$, $b=b_{max}$, $K=K_{min}$ (plant at the bottom of each template in Fig. 5). This is the plant with more difficulties to track the input signal since it represents the biggest load and friction for the smallest motor constant; and it will need the maximum control effort value; this plant is also the nominal plant taken in the QFT design. Nevertheless, the worst saturation effects (higher cost of feedback) occur in the plant with the biggest $|L|$, that is, the plant at the top in the frequency templates of Fig. 5, which corresponds to $J=J_{min}$, $b=b_{min}$ and $K=K_{max}$. Figure 6(a) shows an acceptable tracking performance for $J=J_{max}$, $b=b_{max}$ and $K=K_{min}$, whereas the sensor noise is highly amplified at the control input as Fig. 6(b) shows; it would be even worse for $J=J_{min}$, $b=b_{min}$ and $K=K_{max}$. In practice, this huge cost of feedback will saturate the armature core, spoiling the expected performance in Fig. 6(a).

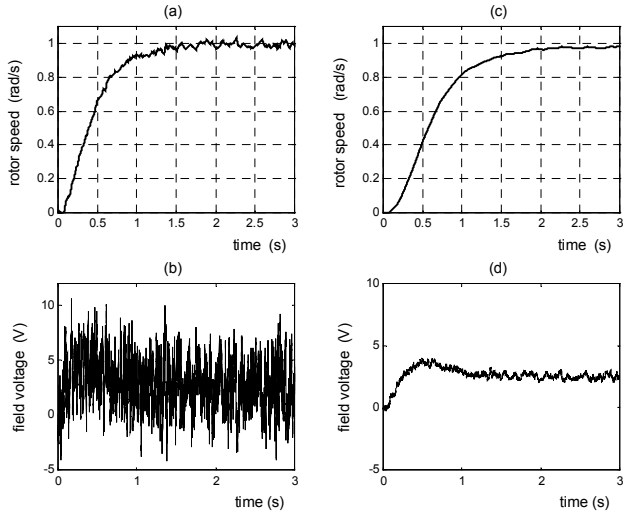

Fig. 6. G_{T1} and G_{T2} output tracking performance, and control efforts, for the plant $J=J_{min}$, $b=b_{min}$ and $K=K_{max}$ in the full uncertainty set

Fig. 3(b) offered a solution to the trade-offs in Figs. 6(a), 6(b). It suggests relaxing the tracking specification values such that $\delta_{Tnew}=\delta_{Tsup}/\delta_{Tinf}=\{1.007,\ 1.375,\ 8.000\}$. Then, the height reduction of the bounds $B(0.1)$, $B(j1)$ and $B(10)$ would allow to reach $|L_0(j100)|<<-20$dB with a controller G_{T2}:

$$G_{T2}(s) = 8\left(\frac{s}{0.8}+1\right)\Big/ s\left(\frac{s}{49.4}+1\right) \quad (6)$$

To complete the control design, the same prefilter that in (5) is used. The cost of feedback reduction shown in Fig. 6(d) compared to 6(b) is not for free. It also implies spoiling the control tracking performance, as shown in Figure 6(c) compared to Fig. 6(a). The solution planned in this paper is the division of the uncertainty.

The J uncertainty contributes strongly to both magnitude and phase uncertainty in the templates at mid frequencies ω_i=1, 10 rad/s. Then, a mere a division of the J domain into two parts may also halve these template uncertainties (see Figs. 5b,c). This ultimately implies a significant reduction of the height of $B(j1)$ and $B(10)$ in the whole phase range $[-2\pi, 0]$ rad (both phase and magnitude uncertainties are reduced). The lowest frequency template (ω_i=0.1 rad/s) is apparently slightly affected by the J uncertainty, which only contributes to its small phase uncertainty (≈0.14 rad in Fig.5a). However, significant bound improvements are gained at the valley points of the bound. Note that the controller has to add an origin pole to avoid tracking static error; then, in the loop-shaping step, the static gain is added nearly at $-\pi/2$ rad, that is, just at the phases with the largest bound relaxation with phase uncertainty division. Then, the benefits may be of interest. J basically contributes to the magnitude uncertainty of the template at ω_i=100 rad/s (see Fig.5d). However, the starting point of the robust-adaptive control planned is just the tracking enhancement, preserving always the robust stability. This forces to compute the high frequency stability bounds with the full uncertainty, dismissing the effect of the J division. Taking all this into account, the rotor inertia uncertainty J=[0.01, 0.1] kg m^2 is divided into two parts: J_1=[0.01 0.05] kg m^2 and J_2=[0.05 0.1] kg m^2. The new plant templates are also depicted in Fig. 5.

New bound arrangements, $B_{J1}(j\omega)$ and $B_{J2}(j\omega)$, at frequencies $\omega=\{0.1,\ 1,\ 10,\ 100\}$ rad/s, are illustrated in Figs. 7(a) and 7(b), respectively. And also the controller designs $L_0(j\omega)$ are depicted, resulting:

$$G_{J1}(s) = 16.2\left(\frac{s}{2.1}+1\right)\Big/ s\left(\frac{s}{26.7}+1\right) \quad (7)$$

$$G_{J2}(s) = 27.7\left(\frac{s}{3.7}+1\right)\Big/ s\left(\frac{s}{18.61}+1\right) \quad (8)$$

Comparing Fig. 7 with Fig. 3(a), the low frequency bound $B(j0.1)$ height improves about –10dB for J_1 and just –3dB for J_2, at the bound valley points (phase $-\pi/2$ rad) where $L_0(j0.1)$ is placed due to its origin pole. Note also the controller static gain reduction in (7) and (8) compared to (4). This will allow at least the same reduction of the high frequency gain $|L_0(j100)|$. Mid frequency ω_i=1 rad/s bound, $B(j1)$, also drops in Fig. 7(a) and Fig. 7(b) compared to Fig. 3(a), thus enabling to place less dominant zeros; see the zero in (4) and the zeros at (7) and (8). This yields a smaller gain increase to be recovered by a pole at a higher frequency. At ω_i=10 rad/s, the bound $B(j10)$ in Fig. 7(a) falls –10dB compared to Fig. 3(a). In the case of the division J_2, the magnitude uncertainty

reduction p_{max}/p_{min} at the ω_i=10 rad/s template drops below the requirement $\delta_T(\omega_i)$ in (*ii*), thus the upper bound B(j10) in Fig. 3(a) relaxes to an outer bound in Fig. 7(b), mainly due to robust stability requirements. In conclusion, $L_0(j\omega)$ in Fig 7(a) can reduce its high frequency gain compared to Fig 3(a), mainly due to the improvement of B(j0.1); meanwhile in Fig 7(b) the benefits are due to B(j10) relaxation. The prefilters for these new designs are the same than the one in (5).

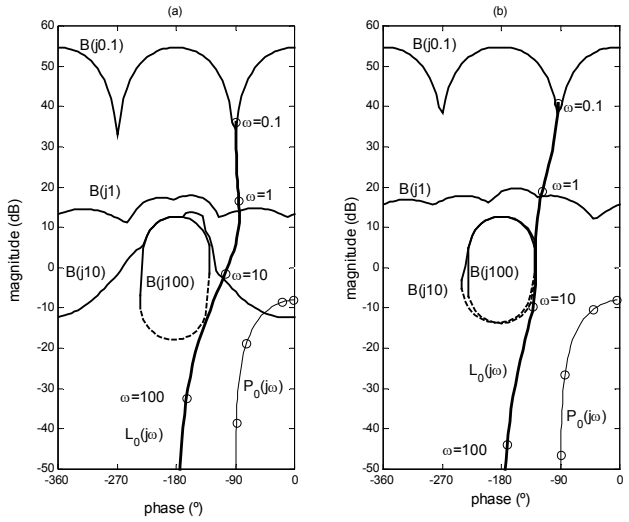

Fig. 7. Bounds and controller designs for uncertainty plant subsets: (a) Division J_1; (b) Division J_2

Fig. 8 verifies the time performance of the new designs. Compare it to Figs 6(a) and 6(c), and note that G_{J1} in (7) equals and G_{J2} in (8) improves the tracking performance yielded by G_{T1} in (4) and, besides, G_{J1} and G_{J2} reduce considerably the cost of feedback. Compared to the performance of G_{T2} in (7), the cost of feedback is now similar whereas the tracking performance is better (see Figs. 6(c) and 6(d) for G_{T2} performance).

5 Conclusions

This paper tackled with the feedback performance limitations for LTI m.p. uncertain plants. Even for these apparently simple to control processes, a high plant ignorance may imply a poor tracking performance in favour of avoiding an excessive cost of feedback, which would saturate the actuators, and guaranteeing an acceptable robust stability. The solution suggested was to carry out a suitable uncertainty division. Different QFT controllers were responsible of maximising the feedback benefits and minimising the cost of feedback in their uncertainty subset. Apart from that, they were robustly stable in the full uncertainty domain. In a further work, a non-linear controller-scheduler structure would be designed. The answer given solves the feedback performance limitations preserving the robustness for plants with arbitrarily large uncertainties.

Acknowledgements

The authors gratefully appreciate the support given by the Spanish 'Comisión Interministerial de Ciencia y Tecnología (CICYT)' under grant DPI'2000-0785.

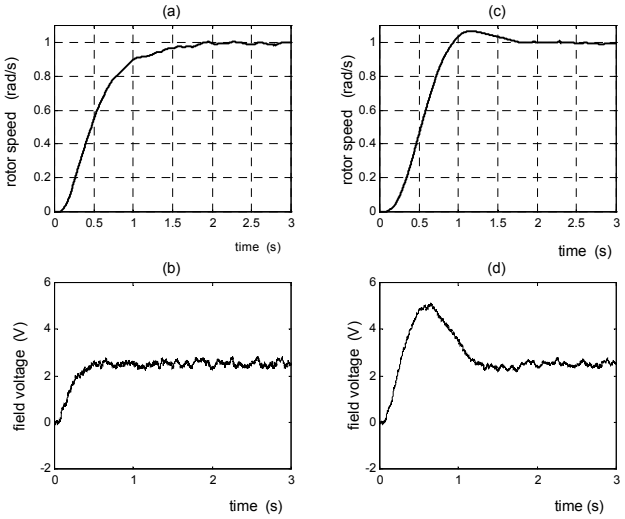

Fig. 8. G_{J1} and G_{J2} output tracking performances and control effort, for the plant $J=J_{min}$, $b=b_{min}$ and $K=K_{max}$ in each uncertainty subset.

References

[1] K.J. Åström, L. Neumann, and P.O. Gutman, "A comparison between robust and adaptive control of uncertain systems," in *Proc. 2nd IFAC Workshop on Adaptive Systems in Control and Signal Processing*, Lund, Sweden, 1-3 July, pp. 37-42, 1986.

[2] K.J. Åström, and B. Wittenmark, *Adaptive control.* Addison Wesley: Reading, MA, USA, 1989.

[3] K.J. Åström, "Limitations on control system performance," *European J. Control*, vol.6, no.1, pp.2–20, 2000.

[4] K.J. Åström, "Model uncertainty and robust control," *Lect. Notes Iterative Identification & Control Design*, pp. 63–100, 2000.

[5] H.W. Bode, *Network Analysis and Feedback Amplifier Design*. Van Nostrand: New York, USA, 1945.

[6] Y. Chait, and O. Yaniv, "Multi-input/single-output computer-aided control design using the Quantitative Feedback Theory," *Int. J. Robust & Non-linear Control*, vol.3, pp. 47-54, 1993.

[7] M. Gil-Martínez, and M. García-Sanz, "Uncertainty fragmentation to reduce static gain in QFT controllers," in *Proc. UKACC International Conference on Control 2000*, University of Cambridge, UK, Sep.2000, pp.151(6 pages).

[8] M. Gil-Martínez, and M. García-Sanz, "Robust specification influence on feedback control strategies." in *Proc. 15th IFAC World Congress on Automatic Control*, Barcelona, Spain, 21-26 July 2002, 6 pages.

[9] M. Gil-Martínez, and M. García-Sanz, "Simultaneous meeting of control specifications in QFT," in *Proc. 5th International Symposium on QFT and Robust Frequency Domain Methods*, Pamplona, Spain, Aug. 2001, pp.193-202. Also accepted for the *Special Issue on Frequency Domain Methods of the Int. J. Robust Control*, expected publication date: 2003.

[10] P.O. Gutman, "Robust certainly equivalence- A new principle for adaptive control," in *Proc.1988 Workshop on Robust Adaptive Control*, Newcastle, N.S.W., Australia, August, 1988, pp. 22-24.

[11] I.M. Horowitz, *Synthesis of Feedback Systems.* Academic Press: New York, 1963.

[12] I.M. Horowitz, and M. Sidi, "Synthesis of feedback systems with large plant ignorance for prescribed time-domain tolerances," *Int. J. Control*, vol. 16, no.2, pp. 287-309, 1972.

[13] C.H. Houpis, and S.J. Rassmussen, *Quantitative Feedback Theory: Fundamentals and Applications*. Marcel Dekker: NY, USA, 1999.

[14] S. Skogestad, and I. Postlethwaite, *Multivariable Feedback Control.* Wiley: New York, USA, 1996; Chap.5-6.

[15] J.R. Wilson, and J.S. Shamma. "Research on gain scheduling". *Automatica,* 36, pp.1401-1425, 2000.

[16] O. Yaniv, P.O. Gutman, and L. Neumann, "An algorithm for the adaptation of a robust controller to reduced plant uncertainty," *Automatica*, vol.26, no.24, pp.709-720, 1990.

[17] O. Yaniv, *Quantitative Feedback Design of Linear and Non-linear Control Systems*. Kluver Academic Publishers: Massachusetts, USA, 1999.